HEAT TRANSFER IN A BLOWN CLOSE-PACKED BED OF FRUIT AND VEGETABLES

M. I. Berman and V. A. Kalender'yan

UDC 532.546:631.576

A system of equations is given for the nonstationary heat and mass transfer in a layer of fruits and vegetables; the numerical solution is analyzed.

Fruit and vegetables are usually cooled in close-packed layers. A good mode of organization is with cooling air blown through the layer and along the side [1, 2]. Then linked heat transfer and moisture transport occur under these conditions, with the water loss by the product, the time to cool to a given temperature, and the temperature and water distributions in the layer are affected.

Any analysis of the regularities in cooling and storage must be based on the theory of heat and mass transfer in close-packed dispersed beds [3, 4]. However, most of the existing methods [1, 2] are based on integral balance equations and are concepts such as the amount of heat per ton of product, which do not allow one to perform a correct analysis even qualitatively.

In some papers [5-8], cooling and storage have been described by examining the local regularities in heat and mass transfer. Here no allowance was made for the heat and water transport normal to the air infiltration speed, or for the contact thermal conduction between components, the heat of respiration, and various other factors, so the recommendations are of limited value [5-8].

Here we consider the heat and mass transfer in a close-packed layer of height H blown in the direction y by air supplied through the bottom horizontal section of the layer of width 2L, whose depth greatly exceeds 2L. The side surfaces of the layer are blown by air entering through slot channels of width $2L_c$. The temperature of the layer at the start T_{t00} differs from the air temperatures at the inlet to the layer and in the side channel T_{i0} and T_{c0}, so there are nonstationary coupled heat and mass transfer processes. With unchanged air inlet parameters, the temperature and the water distributions tend to certain stationary or equilibrium values.

We use a two-component model of interpenetrating media (gas and solid) in the description. Each component is considered as a quasihomogeneous medium characterized by effective transport coefficients that differ in the longitudinal direction y and the transverse one x. The effective thermal conductivities for the solid incorporate conduction through the particles (elements of the bed) and through the contacts and the gas layers between them, as well as radiation; those for the gas component incorporate conduction, radiation, and convection, the last being due to gas mixing in the bed. The effective diffusion coefficient in the gas component incorporates the concentration-dependent diffusion and the convective component. The mass-transfer resistance within the elements is taken as negligible. The heat and mass transfer between the solid and gas components in the bed and also between the air and the side surfaces is incorporated by means of the corresponding heat- and mass-transfer coefficients.

The heat produced by biological processes (respiration heat) is considered as an internal positive heat source in the solid component. The contribution from the respiration heat becomes appreciable under quasistationary conditions and increases as the air infiltration rate decreases. The latent heat of evaporation is incorporated as a heat sink at the surfaces of the particles.

The nonstationary heat and mass transfer may be described on this model via the following system of differential equations derived from the laws of energy and mass conservation:

Odessa Refrigeration-Industry Engineering Institute. Translated from Inzhenerno-Fizicheskii Zhurnal, Vol. 50, No. 2, pp. 266-272, February, 1986. Original article submitted November 14, 1984.

0022-0841/86/5002-0197$012.50

energy for the solid and gas components of the layer

$$(1-\varepsilon)\rho_s c_s \frac{\partial T_s}{\partial t} - \tilde{\lambda}_{s_x} \frac{\partial^2 T_s}{\partial x^2} - \tilde{\lambda}_{s_y} \frac{\partial^2 T_s}{\partial y^2} - \alpha a_s (T_a - T_s) -$$
$$- \rho_s (1-\varepsilon) q_r \exp(bT_s) + \beta a_s q_e [f(T_s) - Ed_a] = 0; \quad (1)$$

$$\varepsilon \rho_a c_{p_a} \frac{\partial T_a}{\partial t} + c_{p_a} G \frac{\partial T_a}{\partial y} - \tilde{\lambda}_{a_x} \frac{\partial^2 T_a}{\partial x^2} - \tilde{\lambda}_{a_y} \frac{\partial^2 T_a}{\partial y^2} + \alpha a_s (T_a - T_s) = 0; \quad (2)$$

mass transfer for the gas comopnent in the layer

$$\varepsilon \rho_a \frac{\partial d}{\partial t} + G \frac{\partial d}{\partial y} - \rho_a \tilde{D}_x \frac{\partial^2 d}{\partial x^2} - \rho_a \tilde{D}_y \frac{\partial^2 d}{\partial y^2} - \beta a_s [f(T_s) - Ed] = 0; \quad (3)$$

energy for the air in the side channel

$$\rho_a c_{p_a} L_c \frac{\partial T_c}{\partial t} + c_{p_a} G_c L_c \frac{\partial T_c}{\partial y} + \alpha_1 (T_c - T_{s_1}) = 0; \quad (4)$$

and mass transfer for the air in the channel

$$\rho_a L_c \frac{\partial d_c}{\partial t} + G_c L_c \frac{\partial d_c}{\partial y} + \beta_1 (d_c - d_i) = 0. \quad (5)$$

If there is an uneven velocity profile in the air at the inlet, or uneven porosity in the bed, one should add the equations of continuity and for motion of air in the layer to (1)-(5). Here we consider a uniform velocity distribution, with the porosity constant. The boundary conditions for (1)-(5) are

$$t = 0 \quad T_s = T_{s00}, \quad T_a = T_{a00}, \quad d = d_{00}, \quad T_c = T_{c00}, \quad d_c = d_{c00}; \quad (6)$$

$$y = 0, \ 0 \leqslant x \leqslant L \quad \frac{\partial T_s}{\partial y} = 0, \ T_a = T_{a_0}(t), \ d = d_0(t);$$

$$y = H, \ 0 \leqslant x \leqslant L \quad -\tilde{\lambda}_{s_y} \frac{\partial T_s}{\partial y} = \alpha_2 a_2 (T_s - T_{a_2}), \quad \frac{\partial T_a}{\partial y} = 0, \quad \frac{\partial d}{\partial y} = 0;$$

$$x = 0, \ 0 \leqslant y \leqslant H \quad \frac{\partial T_s}{\partial x} = 0, \quad \frac{\partial T_a}{\partial x} = 0, \quad \frac{\partial d}{\partial x} = 0;$$

$$x = L, \ 0 \leqslant y \leqslant H \quad -\tilde{\lambda}_{s_x} \frac{\partial T_s}{\partial x} = \alpha_{s_1} a_{s_1} (T_{s_1} - T_c), \quad -\lambda_{a_x} \frac{\partial T_a}{\partial x} =$$

$$= \alpha_{a_1} a_{a_1} (T_{a_1} - T_c), \quad -\tilde{D}_x \frac{\partial d}{\partial x} = \beta_1 a_{a_1} [f(T_{r_1}) - Ed_c];$$

$$y = 0 \quad T_c = T_{c_0}(t), \quad d_c = d_{c_0}(t).$$

In writing (1)-(6), we have neglected the changes in temperature and water content normal to y and x, i.e., we consider the two-dimensional case; we have taken the heat-transfer conditions as identical at both side surfaces; the heat production rate by respiration was taken as varying exponentially with T_S [1]; the mass transfer at the surface followed Dalton's law; and (4) and (5) were written in the one-dimensional approximation for the air in the side channels.

To derive the functions appearing in (1)-(5), we used a finite-difference method, where various constraints were imposed to simplify the system: 1) the side surfaces were taken as impermeable to water, so (5) was eliminated, 2) the thermophysical characteristics of the components were taken as independent of temperature, and 3) the terms incorporating the heat of respiration and $f(T_S)$ were linearized over the possible range in T_S.

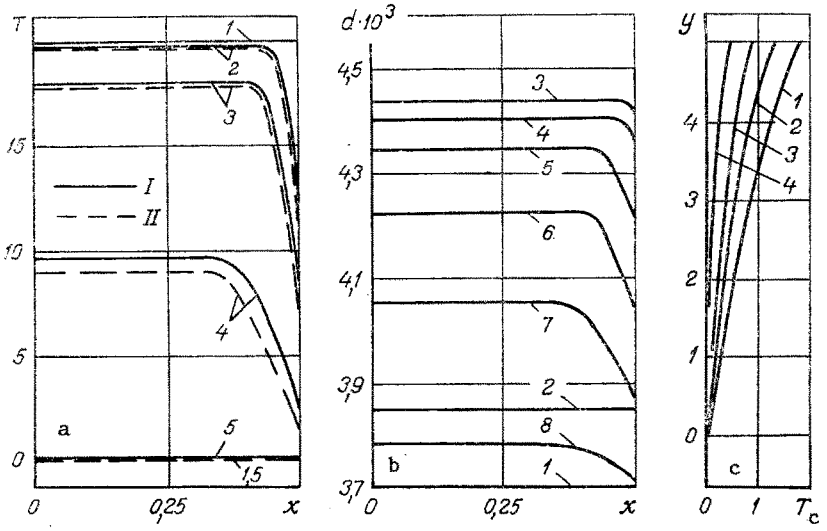

Fig. 1. Variation in time in the temperature and water distributions derived from (1)-(6): a) distributions of T_s and T_a for y = 1 m, I) T_s; II) T_a; 1, 2, 3, 4, 5) t = 0; 0.76; 2.03; 5.39; 14.3 h; b) distribution of d for y = 1 m; 1, 2, 3, 4, 5, 6, 7, 8) t = 0; $2.8\cdot10^{-4}$, $9.9\cdot10^{-3}$; $3.6\cdot10^{-2}$; 0.103; 0.28; 0.76; 2.03 h; c) distribution of T_c over channel height 1, 2, 3, 4) t = 0.28; 0.76; 2.03; 5.39 h; x in y in m, T and T_c in °C, d in kg/kg.

Then (1)-(6) becomes a system of algebraic equations consisting of four subsystems. This system was solved by an iteration method. In each time layer, we solved the subsystems at each iteration, and the results for the previous subsystems were used to calculate the difference analogs of the functions appearing in each next subsystem. The functions obtained in a given step were used in the next iteration. When a given degree of similarity was obtained between successive iterations, we transferred to the next time step.

A locally one-dimensional method [9] was used to solve the two-dimensional equations (1)-(3), which enables one to use an economical calculation scheme. The difference equations were solved by means of an inexplicit pivot method. This enabled us to use fairly large time steps.

The computations were implemented in a FORTRAN program for the ES computers. Preliminary machine experiments showed that the conditions characteristic of cooling and storing fruit and vegetables provided stability in the computation if one chose the conditions for exit from the iterative loops appropriately, together with the initial time step and the mode of alteration in it. We checked for convergence by comparing the results for decompositions of the cross section H × L of the bed into 15 × 15, 20 × 20, 30 × 30, and 20 × 40 nodes, which showed that the results are in agreement as the number of nodes increases and hardly differ one from another as between the 20 × 20 and 30 × 30 cases.

To illustrate the method, we consider the temperature and water-content patterns in a bed of applies with $d_s = 5 \times 10^{-2}$ m, H = 5 m, 2L = 1 m, and depth 1 m. The flow rate of the cooling air at the inlet was $G = 10^{-1}$ kg/m²·sec, with $2L_c = 2 \times 10^{-2}$ m, and G_c = 25 kg/m²·sec in the channel. The parameters of the air at the inlet to the bed and in the channel were taken as independent of time: $T_{a0} = T_{c0} = 0°C$, $d_0 = d_{c0} = 3.7\cdot10^{-3}$ kg/kg; the initial temperature and water-content distributions in the bed were taken as uniform: $T_{s_{00}} = T_{a_{00}} = 20°C$, $d_{00} = d_e$ ($T_{s_{00}}$). The physical characteristics were taken from [1]. The heat-transfer coefficient at the side surface was determined from the curves of [10] for a slot channel, while the coefficient of heat transfer between components and the effective diffusion coefficients were taken from [3], with the component heat-transfer coefficients from [1]. The effective thermal conductivities of the solid and gas components were calculated from [11].

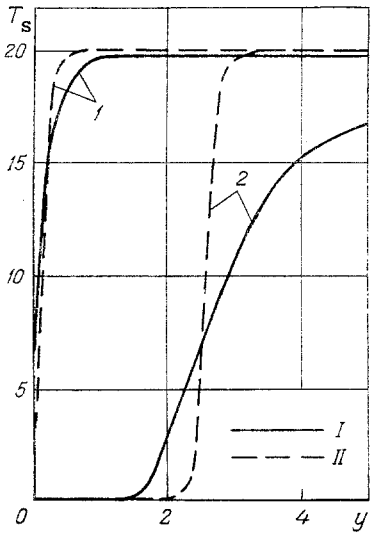

Fig. 2

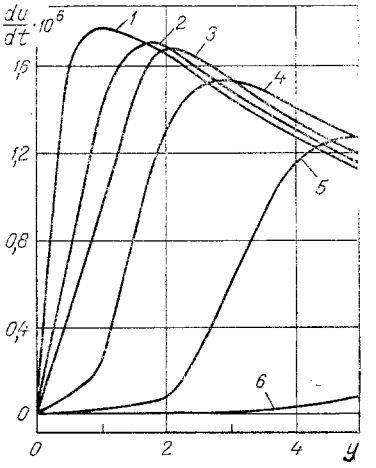

Fig. 3

Fig. 2. Variations in time of the temperature distribution over the height of the bed from the central section x = 0; I) calculation from (1)-(6); II) calculation from [5]; 1 and 2) t = 0.76 and 14.3 h; T_s in °C.

Fig. 3. Variation in time in the distribution over the height of the bed for the rate of local water loss by the product for the central section x = 0; 1, 2, 3, 4, 5, 6) t = 0.103; 0.76; 2.03; 5.39; 14.3; 39.0 h; du/dt in kg/sec·m³.

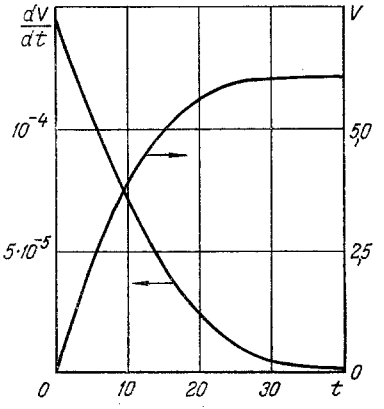

Fig. 4. Time dependence of the integral water loss by the product V and dV/dt; V in kg, dV/dt in kg/sec, t in h.

For each time step, we obtain two-dimensional matrices for the values of T_s, T_a, and d and for the one-dimensional T_c matrices. Figure 1 shows the distributions over the bed (Fig. 1a and b) and over the height of the side channel (Fig. 1c) at various instants. There is marked nonuniformity in the temperature and water-content distributions for the air in the bed (Fig. 1a and b), which is due to the heat and mass transfer in the transverse direction. There is also nonuniformity in the longitudinal direction (Figs. 1c and 2).

The calculations enable one to examine the water loss at various points (in different cells). The values of $u_{ij}(t_c)$ were determined as the increments in the amount of water in the air on passage through a region bounded by the nodes (i − 1, i; j − 1, j) in time $(t_k - t_{k-1})$; the total amount of water lost by the bed up to time t_{N_k} from the start was determined as $\sum_{k=1}^{N_k} \sum_{j=1}^{N_j} \sum_{i=1}^{N_i} u_{ij}(t_c)$.

Figure 3 indicates that there is a maximum in du/dt over the height, which is due to interaction between the water loss, cooling, and saturation of the cooling air on passage through a bed. As time passes, the zone of maximal water loss rate migrates from the inlet section (y = 0) towards the exit one (y = L).

Figure 4 shows that the integral loss rate dV/dt for the product in the volume H × L × 1 attains its maximum almost instantaneously after the start, after which the rate falls exponentially. The integral loss V increases exponentially.

Forms of calculation by this method differ from those of [1, 2, 5-8] in enabling one to analyze in more detail the effects on the local and integral characteristics from various factors involved in a sound choice of optimum cooling and storage conditions. For example, one can compare the calculations on the temperatures with the data obtained for the same conditions from the recommendations of [5], which shows (Fig. 2) that there are both qualitative and quantitative discrepancies, which increase with time, and which occur mainly because the one-dimensional problem was considered in [5], i.e., there was no allowance for transverse transport, whose effects on the temeprature pattern and water loss are important.

The model and method can be used in analyzing coupled heat and mass tranfer in a two-dimensional close-packed layer with internal heat production.

NOTATION

a, specific surface, fraction of surface area; b, coefficient; c_p, heat capacity; d, air moisture content; d_t, particle diameter; D, moisture diffusion coefficient in air; E, coefficient; f(T), dependence of equilibrium air moisture content on temprature; G, mass air velocity; H, bed height; 2L, width; N, natural number; q_r, specific respiration heat; q_e, latent heat of evaporation; t, time; T, temperature; u, V, local and integral moisture loss in bed; x, y, transverse and longitudinal coordinates; α, heat-transfer coefficient; β, mass-transfer coefficient; ε, void fraction, fraction of the cross section; λ, thermal conductivity; ρ, density. Subscripts: s, particle material, solid bed component; a, air; c, channel; e, equilibrium; 0, lower boundary; 1, lateral boundary; 2, upper boundary; 00, initial value; i, j, number of grid node in the x, y direction; k, number of the step on the time coordinate, ($\sim$), effective value.

LITERATURE CITED

1. V. Z. Zhadan, Thermophysical Principles of Storing Harvested Plant Materials at Food-Processing Factories [in Russian], Pishchevaya Promyshlennost', Moscow (1976).
2. I. G. Chumak, V. P. Chepurnenko, and S. G. Chuklin, Refrigeration Installations [in Russian], Letkaya i Pishchevaya Promyshelnnost', Moscow (1981).
3. M. É. Aérov, O. N. Todes, and D. A. Narinskii, Equipment with Stationary Granular Beds [in Russian], Khimiya, Leningrad (1976).
4. V. A. Kalender'yan and V. V. Kornaraki, Heat Transfer and Drying in a Moving Close-Packed Bed [in Russian], Vischa Shkola, Kiev (1982).
5. M. A. Volkov, Heat and Mass Transfer in the Storage of Food Products [in Russian], Letkaya i Pishchevaya Promyshlennost', Moscow (1982).
6. P. M. Dyachek, "The theory of heat and water-exchange processes in the storage of agricultural products," Kholodil'naya Tekh., No. 4, 43-46 (1981).
7. C. D. Baird and J. J. Gaffney, "A numerical procedure for calculating heat transfer in bulk loads of fruits or vegetables," ASHAE Trans., 82, No. 2, 524-540 (1976).
8. V. I. Ivakhnev, E. M. Mal'tseva, and V. N. Rubtsov, "Heat and mass transfer in a bed of fruit or vegetable products with forced ventilation," Mekhanizatsiya i ELektrifikatsiya Sel'skogo Khozyaistva, No. 3, 35-37 (1984).
9. A. A. Samarskii, Theory of Difference Schemes [in Russian], Nauka, Moscow (1983).
10. M. Kh. Ibragimov et al., Turbulent-Flow Structure and Heat-Transfer Mechanisms in Chennels [in Russian], Atomizdat, Moscow (1978).
11. D. Kunii and J. M. Smith, "Heat transfer characteristics of porous rocks," AIChE J., 6, No. 1, 71-78 (1960).